SAND98-2324C

Remote Optical Imagery of Obscured Objects in Low-Visibility Environments Using Parametric Amplification

March 1998 Meeting of the IRIS Specialty Group on Active Systems

Stewart M. Cameron, David E. Bliss, Roy A. Hamil, and Robert B. Asher
Sandia National Laboratories
Albuquerque, New Mexico, 87123

ABSTRACT

The development of unconventional active optical sensors to remotely detect and spatially resolve suspected threats obscured by low-visibility observation conditions (adverse weather, clouds, dust, smoke, precipitation, etc.) is fundamental to maintaining tactical supremacy in the battlespace. In this report, the authors describe an innovative frequency-agile image intensifier technology based on time-gated optical parametric amplification (OPA) for enhanced light-based remote sensing through pervasive scattering and/or turbulent environments. Improved dynamic range characteristics derived from the amplified passband of the OPA receiver combined with temporal discrimination in the image capture process will offset radiant power extinction losses, while defeating the degradative effects of multipath dispersion and diffuse backscatter noise along the line-of-sight on resultant image contrast and range resolution. Our approach extends the operational utility of the detection channel in existing laser radar systems by increasing sensitivity to low-level target reflectivities, adding ballistic rejection of scatter and clutter in the range coordinate, and introducing multispectral and polarization discrimination capability in a wavelength-tunable, high gain nonlinear optical component with strong potential for source miniaturization. A key advantage of integrating amplification and frequency up-conversion functions within a phasematched three-wave mixing parametric device is the ability to perform background-free imaging with eye-safe or longer infrared illumination wavelengths (idler) less susceptible to scatter without sacrificing quantum efficiency in the detection process at the corresponding signal wavelength. We report benchmark laboratory experiments in which the OPA gating process has been successfully demonstrated in both transillumination and reflection test geometries with extended pathlengths representative of realistic coastal sea water and cumulus cloud scenarios. In these experiments, undistorted range-gated optical images from specular and diffuse reflectance targets were acquired through scattering attenuations exceeding ten orders of magnitude which would be undetectable with traditional optical methods. The broadcast and gating pulses were derived from both millijoule 10 Hz picosecond (50-100 ps) and 250 KHz microjoule femtosecond (~150 fs) laser configurations to assess signal-to-noise and spatial resolution considerations as a function of scattering, integration time, and repetition rate. In addition, the technique was combined with a self-referencing Shack-Hartmann wavefront sensor to diagnose underlying phase signatures of weak refractive index gradients (OPD~λ/100) or persistent convective wakes (exhaust plumes, bubbles), and to perform adaptive optical compensation in visual fields exhibiting both turbulence and turbidity (OD=4). Comparative system analysis results relating image quality, optimal gate width, detectable range, and broadcast laser size versus operative atmospheric scattering conditions and search/dwell probability of detection criteria will also be presented.

I. INTRODUCTION

In general, active imaging provides greater spatial discrimination against interference from clutter and thermal loading artifacts with a correspondingly lower frequency of false alarm. The angular resolution associated with laser imaging radars in conjunction with the inherent modulation bandwidth available for pulse shaping of the ambiguity function allows substantial target classification capability including simultaneous bearing, range, velocity, and wavelength-dependent reflectance in a single measurement. Although optical remote sensors have tremendous advantage over other types of analytic sensors in focussing and range resolution characteristics, general application is limited by their inability to operate effectively in the presence of optically thick layers, multiple scattering obscurants, or adverse weather along the propagation axis. To be useful for threat warning and surveillance against time-critical targets, implementation of range-resolved imagery under reduced atmospheric visibility conditions must exhibit immunity to scattering degradation and be adaptable to a broad range of sensing wavelengths to optimize background contrast.

We have developed an innovative frequency-agile image intensifier technology based on optical parametric amplification (OPA) in the receiver channel which integrates multispectral imaging functionality with active short-

DISCLAIMER

pulse ballistic gating in the range coordinate to defeat the cumulative effects of attenuation loss, multipath spatial and temporal dispersion, and diffuse backscatter saturation noise on image capture in the presence of obscuration. Using this baseline approach, standard modelocked lasers at modest pulse energies have been used to acquire undistorted optical images from specular and diffuse reflectance test objects through extended scattering attenuations exceeding ten orders of magnitude (corresponding to approximately 1-3 km of high-altitude clouds or 20 meters of Chesapeake Bay water) with transverse spatial resolution near the diffraction limit. Improved dynamic range characteristics derived from the amplified spectral and spatial passband of the OPA device combined with temporal discrimination in the gating process allow the extraction of images from pervasive scattering backgrounds of hidden objects which would be completely unobservable by conventional optical means. The expanded dynamic range characteristics offset previous limitations on the detectability of low-level returns resulting from multiple scattering or low object reflectivities while preserving full image fidelity. Time-gating in the range coordinate can be used to distinguish closely spaced multiple glints and to segment nearby background clutter or multipath ambiguities from the image resolution cell for precise visualization in complex targetting environments. Speckle reduction may be possible by operating a noncritically phasematched type I parametric process at the degenerate point in the mode of a forward-going three-wave phase conjugate interferometer.

The combination of short-pulse broadcast format with a high gain receiver increases immunity to countermeasures and decreases system size requirements for fixed stand-off distances relative to conventional laser radars, making the overall system implementation compact and amenable to evolving miniaturized pulsed diode laser architectures. Our system improves upon current performance metrics by increasing dynamic range, adding scatter rejection and range resolution, and by introducing the flexibility to frequency-upconvert images generated with eyesafe or longer infrared illumination wavelengths to visible wavelengths detectable with high quantum efficiency within the silicon photocathode response envelope. In particular, by working in the eye-safe spectral region below human visual response, but above the short-wavelength cut-off for most passive infrared systems, a favorable compromise between atmospheric propagation and extinction effects can be balanced against minimum broadcast energy and risk of detection. The ability to tune the OPA receiver bandpass over multiple spectral signature regions to optimize target-to-background contrast permits exploitation of genetically-based or neural net visual perception image algorithms to further optimize measurement content regarding shape recognition and movement, and can reduce the need to employ sub-pixel processing in the CCD plane. By overcoming the effects of turbidity and clutter on image resolution and range accuracy, this technology substantially augments the scope of existing surveillance radars and expands the existing RSTA (reconnaissance, surveillance, target acquisition) and counterforce mission profile to include severe uncontrolled field conditions where either direct line-of-sight imagery or millimeter wave is inadequate under theatre rules of engagement to support precision aimpoint selection or to accomplish accurate battle damage assessment in the post-strike debris field. This approach will also provide a basis for a covert, extended-range wide-bandwidth optical communication system which can be adapted to transmit and receive undistorted data streams from an autonomous ground-based distributed sensor array regardless of atmospheric conditions.

Integration of a Shack-Hartmann sensor or phase conjugate "wavefront scrubber" with active temporal gating in an OPA introduces a new diagnostic capability for the detection of translucent phase objects or refractive index wake fields and boundary layers in the presence of turbidity which would be prohibitive for standard interferometric measurements. Moreover by combining adaptive optics methods with OPA ballistic gating, compensation for both atmospheric turbulence and light scattering on image resolution can be accomplished simultaneously. Since the gating process isolates the residual transmitted coherent field from the diffuse background, turbulence-induced phase perturbations and low-frequency optical aberrations superimposed on the propagating return (referenced to a guide star or itself) can be accurately diagnosed in a wavefront sensor downstream of the gate. The measured error signal then becomes the basis for an adaptive compensation feedback loop with a deformable mirror.

II. TECHNICAL APPROACH AND CONCEPT OVERVIEW

• *Effects of Scattering on Range-resolved Optical Imaging*

The primary obstacle to to implementation of light-based imaging in low-visibility environments exhibiting pervasive scattering is the presence of spatial and temporal dispersive effects induced by the random scattering process itself which can mask the direct optical line-of-sight. Multiple diffuse scattering acts as a fog to produce a broad distribution of optical propagation delays and irregular, randomized photon trajectories thereby degrading underlying image information and progressively scrambling the geometrical correlation between incident and detected light. Optical dispersion induced by multiple scattering from turbid meterological and artificial obscurants such as fogs (clouds), aerosols, dust, haze, smoke, and precipitation can produce a broad temporal distribution of multipath delays superimposed on a strong diffuse light background as a function of scattering anisotropy $g(\cos\theta)$,

cross section κ, and particle albedo. The resulting pathlength uncertainty associated with the detected signal will adversely affect quantification of absorbance and the accuracy of range-resolved optical sensing measurements derived as a function of delay time. Concomitant spatial dispersion will enlarge the corresponding point spread function defining image quality and resolution, and optical attenuation of the radiant power will decrease received signal strength. In addition, the diffuse scattering background level will reduce effective dynamic range and maximum stand-off distances available for unambiguous object detection and classification. When the object visibilty is indistinguishable from the diffuse background, the scattering layer effectively becomes opaque to the observer. Turbulent flow and random index variation associated with inhomogeneous mixing of thermal layers can refractively deform the incident laser beam introducing pathlength error (phase noise), beam wander, and beam distortion which also effects spatial localization.

• ***Ballistic Time-Gating Method***

Ballistic imaging is a path-sensitive coherent imaging approach designed to overcome the degradative effects of turbidity on traditional line-of-sight optical imaging methodologies by exploiting the influence of scattering inhomogeneities on the temporal dynamics of photon diffusion [1]. This technique seeks to temporally isolate image information from the adverse effects of multiple scattering using an ultrafast optical gate (nominally < 100 ps) superimposed on the transmitted or reflected time-of-flight distribution to preferentially detect so-called ballistic (minimally scattered) photons which obey geometric optics and exhibit diffraction-limited resolution.

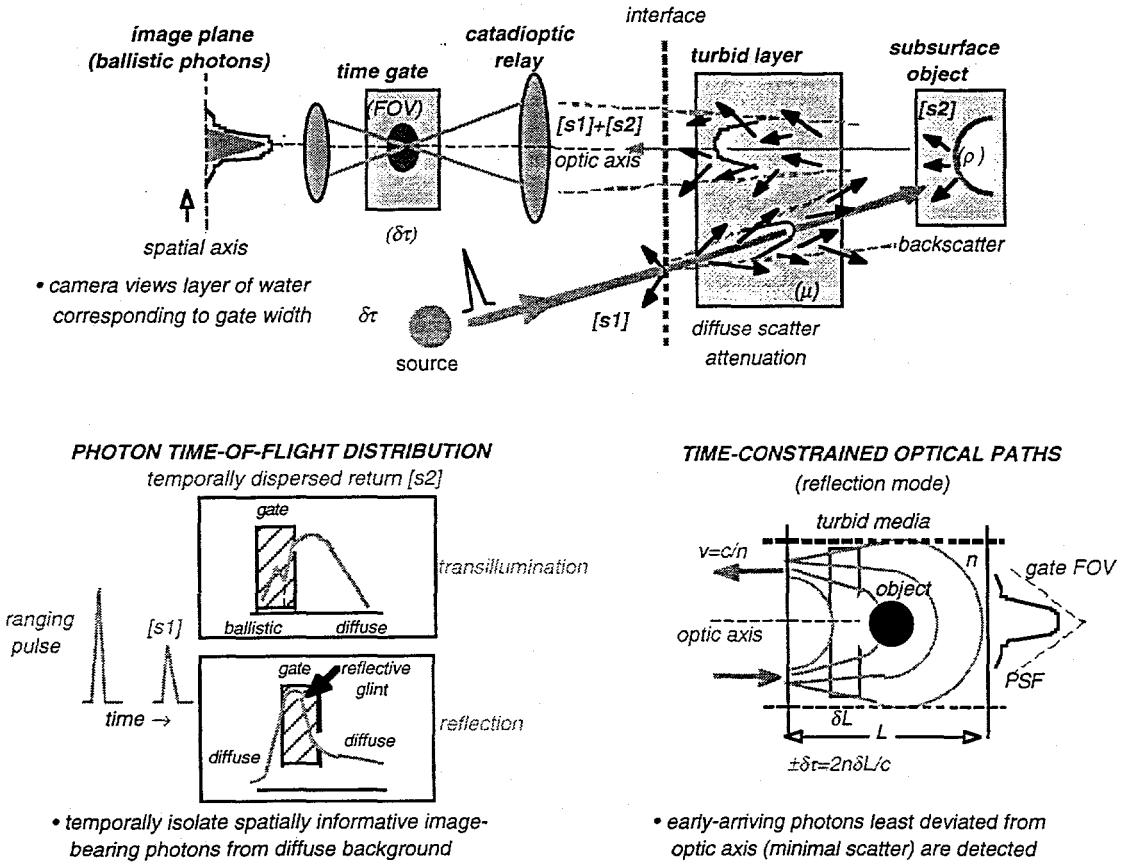

Figure 1: Ballistic imaging is a coherent path-sensitive approach which seeks to compensate for adverse "fog-like" effects of scatter on image formation in turbid media. The influence of scattering on the temporal and spatial dynamics of photon diffusion can be exploited to capture an obscured image and defeat background light.

The conceptual idea behind time-resolved measurements of this general type is to constrain the distribution of possible light paths and corresponding field-of-view to those relatively rare first-arriving paths exhibiting marginal deviation from the optic axis. These spatially localized paths result from the coherent interference of light scattered in the forward direction and propagate essentially undeviated by scattering events with the least distorted image information. By introducing time-resolved detection to select a certain fraction of these early photons for analysis and eliminating the bulk of the integrated diffuse scattering contribution, only the most spatially informational photons relevant to image capture are detected which effectively sharpens the point spread function defining image quality and

spatial resolution. Temporal gating combined with spatial frequency bandpass rejects or filters out the much larger number of late-arriving photon trajectories which follow long random walks resulting from incoherent diffuse scattering through the medium. By eliminating the scrambled incoherent photons (blur) appearing as background noise in the image plane, optical pathlength uncertainty over the gate interval contributing to range error is avoided. Note the fundamental difference between reflection and transmission modes in the imaging problem. In the transmission case (single pass), the earliest arriving light is unambiguously the quasi-ballistic image-bearing component and gate position for optimal image quality is strictly a monotonic function of propagation delay. However, for the reflection case, diffuse scattering occurs both on the incoming and outgoing paths so that the requisite time-gate position for best image resolution must be actively scanned to find the correct originating glint boundary. This has important consequences for search and dwell protocol, the so-called "needle-in-a-haystack" problem, and for SNR considerations and visibility threshold in the practical case of reconstructing three-dimensional extended objects. Overall transverse image quality is generally worse for the reflection than the transillumination (or shadowography) case because of beam spread during propagation to the target plane which creates a degraded initial condition for the return process.

Numerous experimental methods to implement the requisite temporal discrimination have been demonstrated including optical shutters based on transient nonlinear Kerr[2], photorefractive[3], or stimulated Raman interactions[4], "light-in-flight" interferometric[5] and cross-correlation heterodyne/homodyne gating[6] based on field coherence properties, electronically gated streak camera imaging[7], and time-correlated single photon counting[8]. Practical remote sensing issues regarding laser intensity, optical complexity, wavelength-tunability, signal processing, packaging, and phase distortion in atmosphere have limited robustness for application. In our approach to ballistic imaging, we will incorporate a frequency-agile OPA time-gate[9,10,11] which simultaneously exhibits both spectral and spatial (angular) passband characteristics for amplified image transfer through extended scattering environments.

• ***Optical Parametric Amplication***

Although ballistic imaging can show close to diffraction-limited performance, previous incarnations of the technique suffered from extremely small signal levels due to the selective nature of the time-gating process which discarded the bulk of the illumination energy to achieve maximum image contrast. To circumvent these practical limitations, the authors have demonstrated a novel wavelength-tunable, short-pulse amplifying gate functionalized for ballistic imaging applications based on optical parametric amplification. Parametric amplification, also referred to as difference mixing generation, is of particular interest not only because it is a gain process which can defeat small-

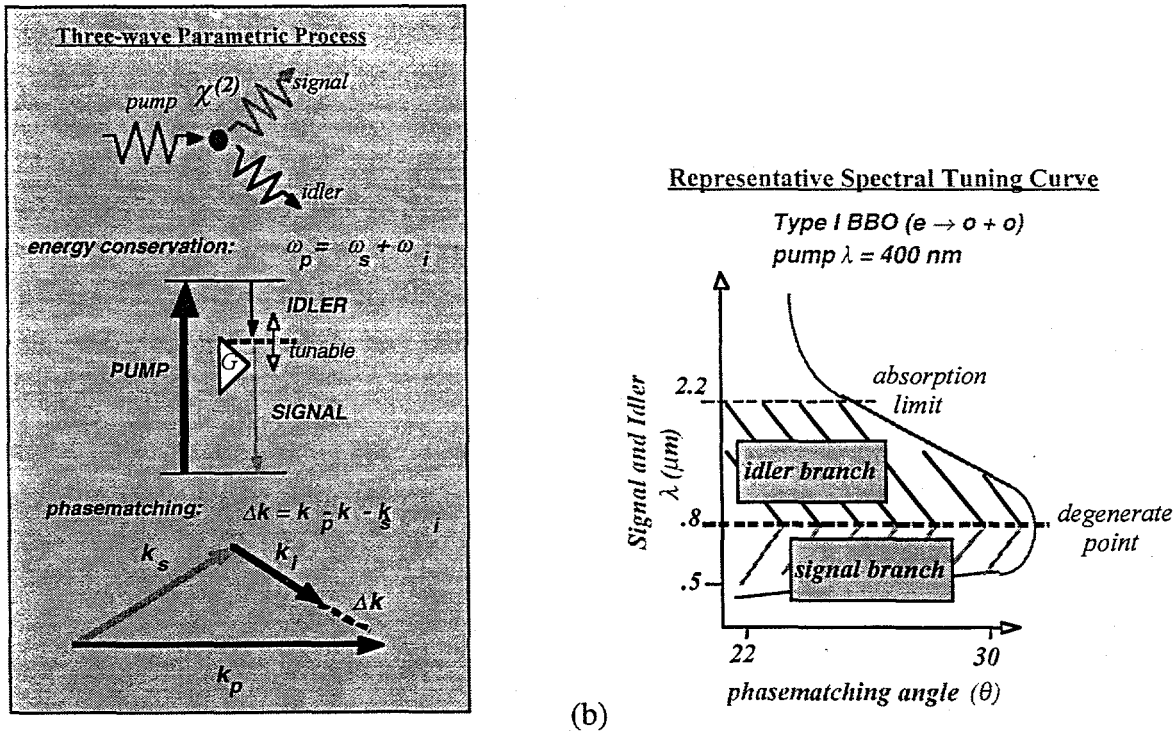

Figure 2: Basic Physics Overview of the OPA process (a) Pump photon generates signal and idler photons subject to energy and phasematching constraints, (b) Representative spectral tuning curve.

signal detection limitations from low reflectivity objects, but also because the time during which amplification occurs can be effectively limited by the duration of an applied pump (gating) pulse to preserve maximum range resolution and to reject diffusely scattered light detrimental to image contrast.The OPA process accomplishes substantial discrimination against time-delayed diffuse scattering while maintaining high transmission efficiency of the coherent component. An optical parametric amplifier is capable of fast temporal gating, direct two-dimensional image acquisition and spectral conversion over a broad wavelength range defined by the signal/idler tuning curve, quantum sensitivity approaching one photon per spatial resolution element, and a high degree of coherent discrimination against diffuse light obscuration of image quality.

As shown schematically, the gating mechanism involves the temporal and spatial overlap of a strong reference (gating) beam with the attenuated image-bearing probe beam in a phasematched nonlinear crystal to produce gain via a three-wave parametric $\chi^{(2)}$ interaction on both the signal (visible) and idler (infrared) branches. In this process, each incident pump photon pairwise generates two tunable lower frequency photons denoted signal (ω_s) and idler (ω_i) subject to momentum and energy conservation conditions with gain scaling dependent on the crystal interaction length (L) and nonlinearity (d_{eff}), pump intensity (I_p), and phase mismatch (Δk). The gate acts as a noiseless image intensifier (in the absence of spontaneous parametric scattering) to simultaneously amplify and temporally isolate the weak quasi-ballistic or early-arriving partially coherent component of the transmitted light. Gain in the amplifier exists for approximately the duration of the pump pulse and the nature of the nonlinear optical coupling- primarily the time correlation, angular acceptance, and phasematching- provides temporal, spatial, and polarization discrimination against diffusely scattered background light. The resulting polarization sensitivity in the parametric process may be useful for polarimetric differentiation between man-made and natural structures, and for foliage penetration. Note that a quantum amplifier cannot improve the inherent input SNR associated with a faint object (in the absense of squeezing), but it can prevent further degradation of the signal caused by low quantum efficiency of the detector and allow attainment of unity signal-to-noise with minimum broadcast size depending on the noise equivalent power (NEP) described below. In this sense, the OPA may be useful as a preamplifier in wide bandwidth receiver applications which have traditionally sacrificied gain for detector time response.

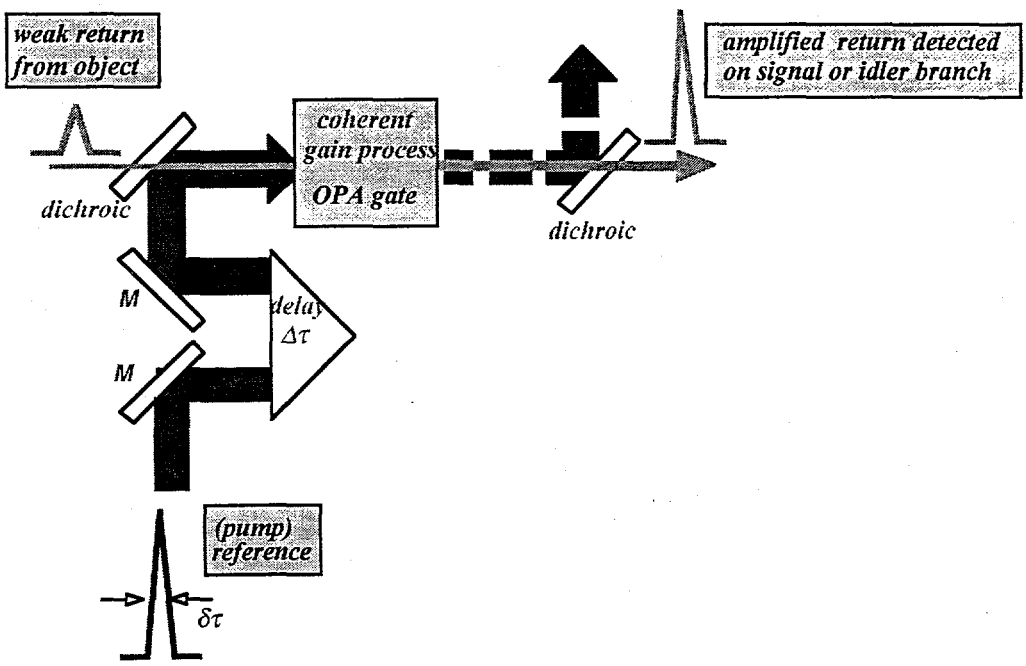

Figure 3: Schematic of an optical parametric amplifier realized as an image intensifier for range-gated detection. Energy from the synchronous pump beam is transfered to the signal and idler branches such that energy and phase in all three coupled waves is conserved and gain is possible. Optical gate simultaneously amplifies and temporally isolates ballistic image. Polarization attributes defined by phasematching geometry.

Difference frequency in an OPA device can provide gain as well as versatile spectral tuning by virtue of the parametric coupling process between incident optical fields. Broad wavelength tuning can be accomplished over the signal/idler tuning curves by systematic angular variation of the crystal phasematching conditions to minimize momentum mismatch and maximize gain subject to energy conservation for the specific nonlinear crystal used in the gate. As an example, for the case of type I β-barium borate (BBO), spectral tuning is possible with suitable dichroic

coatings from the blue-green ~450 nm to 2.2 μm (absorption limit) using a 400 nm pump wavelength and a single angle-tuned crystal (28° cut). We have observed unsaturated gains $>10^5$ for fixed pump intensity over this range and a corresponding spectral bandpass $\Delta\nu \sim 10$ cm^{-1}. Range profiling is accomplished by monitoring the transmitted amplitude during the optically-delayed amplification interval set by the gating pulse width $\Delta\tau$.Transverse spatial resolution is determined by the spatial magnification of the gating pulse for the specific crystal focussing geometry defining the gain region, and the longitudinal (range) resolution is fixed by the incident pulse duration $\delta\tau$. Contrast of the gate is defined by the ratio of light transmitted when the reference beam is present to the off condition. The active nature of the time-gating process requires that the pump beam (which does not leave the local laser transmitter environment) must be accurately synchronized to overlap with the reflective edge of the dispersed return for effective gain transfer.

III. OPERATIONAL ISSUES

• ***Laser Miniaturization***

(U) Because the OPA gate nonlinearity is inherently based on a low-order $\chi^{(2)}$ pumping process and exhibits high gain, system scaling is compatible with the use of sub-nanosecond passively switched diode-pumped microchip laser designs developed at MIT Lincoln Laboratories as a pump source[12]. These compact solid-state sources exhibit high brightness and spatial coherency, and maintain sufficient energy margin to penetrate relatively thick scattering layers. The peak power in these devices is sufficient to drive nonlinear devices such as OPOL/OPAL and PPLN-based parametric amplifiers for frequency conversion and range-gating applications. In particular, diode pumped lasing and optical parametric interactions can occur in the same crystal enclosed inside overlapping resonantors with high efficiencies due to good mode matching. Photoconductive semiconductor switch (PCSS) technology can also be used as a short-pulse pumping mechanism for gain-switching laser diode arrays and for generating fast electrical transients ~250 ps to trigger saturable absorbers or Q-switches in a hybrid microchip resonator to reduce timing jitter[13]. A laser diode array with a PCSS has been recently constructed at Sandia National Laboratories, NM which generates sub-nanosecond >100 μJ gain-switched pulses at 10 KHz (variable). Several authors have reported high-power, diode-pumped Nd:YAG picosecond regenerative amplifier designs incorporating an intracavity KTP OPO which are capable of generating ~25 ps pulses with nominal 100 μJ energies at 1.54 μm [14].

• ***Search and Dwell- "Needle in a Haystack problem"***

It is important to note that the active nature of the time-gating process, as compared to a scannerless design with a passively modulated receiver, requires the gating pulse to be accurately synchronized to overlap with the reflective edge of the dispersed return for effective gain transfer and image acquisition in the OPA. This is a necessary condition to overcome the degradative effects of light scatter and background clutter on ranged-imaging, but limits the effective depth of field of a single frame to the gate pulse width. As a result, the gate delay must be scanned to an accuracy of the pulse length to acquire the initial image and then slewed in time or discretely multiplexed with a formatted pump pulse to build up sequential images over the entire range field. In the absence of supplementary queing sensor data, this puts a constraining condition on the broadcast laser repetition rate (prf) in relation to the platform velocity, allowable search time, extent of object, and gate width (range resolution) to insure 100% probability of sampling a target image or to insure minimal lapses in ground mapping coverage. We can create conditions to guarantee image acquisition with multiple frames at many ranges but not duplicate the continuous depth of field of the scannerless optical radar case. Accurate range tracking over the search area will require continuous (iterative) monitoring of the OPA scan delay or gate position between the transmitted pulse and the range echo from target. Achieving the necessary integration conditions for an acceptable SNR threshold and probability of detection with a given false alarm rate for the operative Swerling model of target phenomenology sets a pulse rate sampling constraint on the broadcast PRF [15].

For this reason, the most likely application of this technology is in a "close-up" zoom mode when exceptional high-resolution reconnaissance accuracy is required as a follow-on to a passive wide-area sensing measurement with scanning field capability or when scannerless systems are degraded by adverse visibility. In the former case, the complimentary aspects of the two systems, passive detection and active spatial localization allows for direct determination of target extent irrespective of emissivity and background loading characteristics which can fool false-color infrared processing. The nonlinear ballistic time-gating process in the OPA receiver can defeat scattering and clutter obscuration of the direct line-of-sight in stressing environments, but comes with the added complexity of a requirement for a synchronizable pump beam to activate the gate at the appropriate delay time(s) in the time-of-flight spectrum. Because the dispersed return through an extended turbid medium such as cloud cover may arrive many microseconds after the inital broadcast pulse, and may require a gatewidth <100 picoseconds for acceptable diffuse scatter rejection in the imaging process, stringent timing precision and stability must be maintained. This is

generally accomplished using programmable pockel cell shutters (nanoseconds) in combination with a precise scanning optical delay line (picoseconds) when the range distance is unknown. A scheme based on this approach using a common modelocked oscillator pulse train and two independently delayed regenerative amplifiers is described in the experimental section.

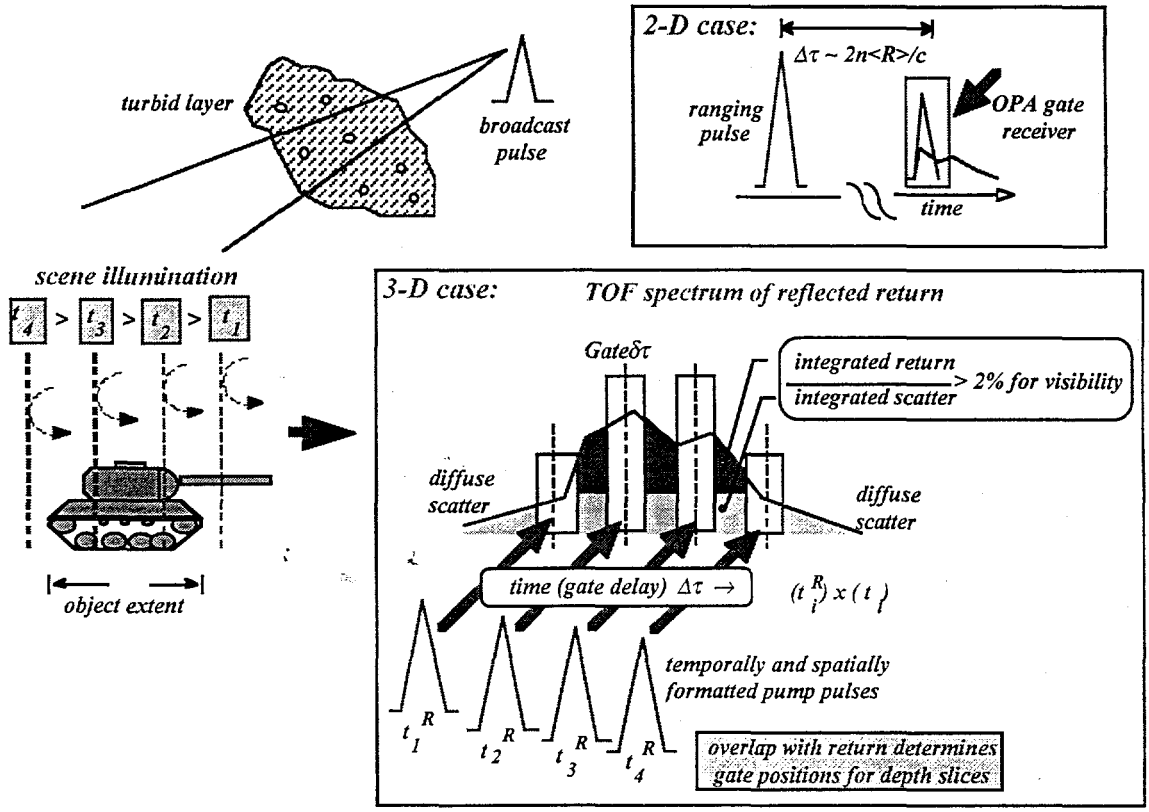

Figure 4: Reconstruction of an obscured 3-D object using formatted pump pulses to multiplex range gates from a single floodlight illumination pulse. Note that a single pulse interrogates the full object profile.

One approach to solving the search and dwell problem associated with limited depth of field in the range coordinate is to field a dual mode monostatic lidar architecture comprised of a one-dimensional low-resolution scanning search radar co-boresighted with a limited angular sector high-resolution tracking optical radar. In implementation, approximate location, Doppler, and heading information of potential targets are obtained by the search radar over a conical swath using standard multiple discrete PRF ranging and coincidence detection (usually Khz submultiple) in the transmit/receive channels. This data is then handed off to the tracking radar which uses an encoded on/off receive gate cycle pattern with variable overlapping widths over the duration of the detection pulse to produce a composite image of ranged pixels; i.e., swept receive gates in multiple OPA gates perform continuous range tracking over the interpulse spacing. Scanning of the laser beam over limited angular extent may be necessary to fully acquire the target and center the range gates prior to lock particularly for the case of evasive maneuvers.

• ***Optimum Gatewidth Determination for Transverse Spatial Resolution: Image Quality Assessment***

A general quantitative expression relating gate width and lateral spatial resolving power of a ballistic imaging system is difficult to determine since it depends on empirical variables such as illumination/detection geometry, scattering properties, and specific evaluation criteria concerning the quality of the time-resolved image. Small changes in the scattering cross section will sensitively affect the optimum delay time for a given level of resolution and the gate width is also expected to change depending on the number of transmitted photons within the integration time necessary to exceed the fundamental shot noise limit of detector response and form an informative image. In general, however, transverse spatial resolution of features located in the midplane of a rectangular scattering medium should be linearly proportional to the maximum possible displacement of photons located within that plane which is a ellipsoid-shaped function constrained by the integration time (gate width). This means that the allowable path deviation from the optic axis along the scattering divergence cone is determined by the gate duration to first order[16]. Theoretical studies based on the diffusion approximation, Monte-Carlo simulation, and random path models have shown that the curve describing transillumination resolution Δx (width of PSF) capability of an

imaging process as a function of integration time $\Delta\tau$ and scattering thickness L follows an asymptotic square root behavior $\Delta x \sim (2c\Delta tL)^{1/2}$. In the absence of detector photon noise, best achievable resolution is theoretically obtained with the shortest experimentally viable gatewidth which is inherently constrained by the combinative effects of illumination dosimetry (broadcast energy) and the fundamental quantum noise of the detector. As the scattering attenuation increases, the practical range of useful gatewidths fulfilling this criteria decreases and the resulting resolution defined as the half-width (1/e) point of the Gaussian point spread function degrades toward the diffuse (no gate) limit ~ $.2L$.

We can roughly approximate the case of reflective imaging as two folded transillumination problems, first in propagation through the scattering layer to the target plane and then reversing direction for the outgoing path with the dispersed input beam as a new initial condition. To account for noise, we use an image quality index (IQI) or predictor based on decision theory that has been developed by radiologists to establish a more rigorous quantitative resolution criterion defining object detectability[17]. This calculation can be performed from knowledge of the line spread function of the imaging system, the noise pattern $W(\Delta t)$ of the image background, and the contrast function $C(\Delta t)$ of the imaged object. In first approximation, the IQI value is proportional to the square root of the sum of Gaussian LSF variance (σ^2) and the white noise amplitude given by the integral of the assumed Wiener spectrum

$$\Delta x \sim 2[\sigma^2(\Delta t) + \gamma \div W(\Delta t) / C(\Delta t)]^{1/2} \qquad (1)$$

with a correcting constant γ which is a function of the estimated signal-to-noise ratio (S/N) for high detection probability (i.e., threshold of detection) and imaging collection geometric factors. Large contrast at short range implies a more robost tolerance for noise in the image (more photons) and the potential for short integration times and high spatial resolution; decreased contrast, longer ranges, or increased noise decreases resolution and increases optimal gate width and image blur. The IQI of an unfocused OPA range gate (excluding spontaneous parametric scattering noise) calculated for a homogeneous scattering thickness L~200 m (κ_{sc} ~.01 m^{-1}) and a 100% diffusely reflecting Gaussian target (contrast=1) with SNR=6 is shown below:

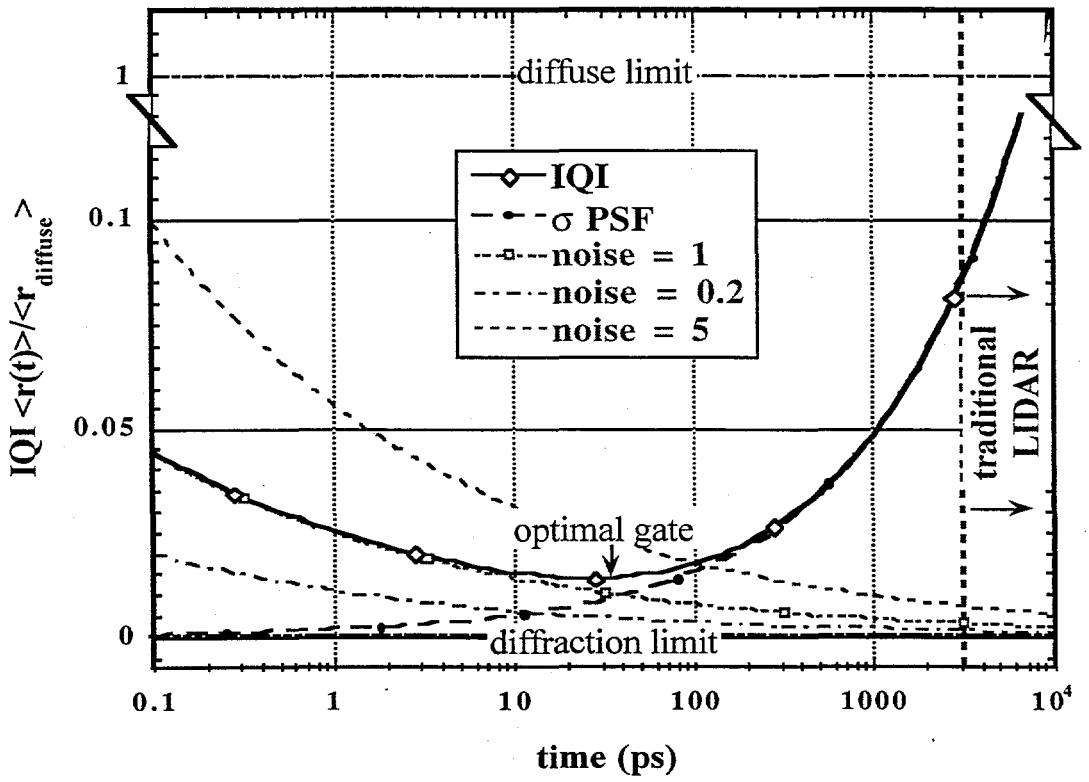

Figure 5: Image quality index or transverse PSF as a function of gate width for range-gated detection through a scattering layer. Comparison with nanosecond lidar and diffuse limit.

Note that the useable signal for very short gate times is strongly occulted by noise as seen by the rapid rise in the IQI as $\Delta t \rightarrow 0$. This non-intuitive behavior can be explained on the basis of the interplay of noise statistics with the sharpening mechanism of the LSF when the time-window goes to zero. Although resolution and image contrast of an obscured object theoretically improve as the integration time is decreased, ideally approaching the pure ballistic limit, the SNR simultaneously decreases due to noise augmentation from superimposed detector quantum statistics which were previously washed out for longer intergation times. As the width of the gating window diminishes, time-resolved detection reduces the number of collected photons and effectively decreases the SNR on each pixel, thereby accentuating noise features which offset the expected gains in image quality.To obtain the best possible compromise between spatial resolution and IQI noise issues, one should use a temporally narrow ranging pulse for maximum achievable spatial resolution in conjunction with a optimizable variable gate width to preserve detectability of the temporally dispersed output. Short pulse ballistic gating in the 10-100 picosecond regime clearly improves the transverse spatial resolution over longer nanosecond exposures in the presence of multiple scattering by limiting the extent of the measured scattering cone. The short pulses will also improve accuracy in the range coordinate but there is no fundamental SNR improvement in the reflectance case for an extended target.

• ***Frequency Upconversion***

Difference frequency in an OPA device can provide gain as well as versatile spectral tuning by virtue of the parametric coupling process between incident optical fields.The resultant image can be observed directly at the incident sampling (broadcast) wavelength (image amplification) or alternatively on a zero background at the spectrally converted difference frequency between pump and probe (sideband image upconversion). A key advantage of combining amplification and spectral conversion functions in a single parametric gate is the ability to perform imaging at longer infrared idler wavelengths less susceptible to diffuse scattering without sacrificing the capability for efficient amplified detection at signal wavelengths within the silicon photocathode response envelope (<1100 nm).The use of a cascaded experimental geometry consisting of a tunable light source transmitter based on parametric amplification in conjunction with a second time-delayed OPA-based ballistic gate in the receiver channel would allow full flexibility in designing an imaging system for turbid backgrounds while matching favorable transmission windows and wavelength-dependent size effects in the Mie scattering function.

• ***Spontaneous Parametric Fluorescence Noise***

An important parameter of any optical detection device is the noise equivalent power (NEP) which measures the amount of noise present in the absence of signal. A fundamental noise source in an optical parametric amplifier is spontaneous parametric scattering or fluorescence occuring as a result of amplification of noise photons initiated by zero-point vacuum fluctuations (noise input per mode of $h\omega/2$ in either the signal or idler channel). This nonlinear emission occurs when the initial number of photons in the signal and idler fields is zero (no seed present), and exhibits a scattering intensity higher than could be explained due to parametric mixing of the incident pump beam with quasi-phasematched blackbody radiation at the signal or idler frequency [18]. Existence of such a phenomenon follows as a necessary consequence of quantization of the electromagnetic fields and the nonlinearity in the susceptibility of the amplifier medium. The superradiant process is a fundamental limit in high gain systems approaching $\Gamma L \sim 20$ and will lead to false images in gating applications operated under these conditions (for our pump and gain conditions, we observed this phenomena at a broadcast to reflective return intensity ratio of $I/I_0 \sim 10^{-11}$). In the near infrared and shorter wavelength range, OPN dominates the thermal noise $P_{th} \sim h\omega[\exp(h\omega/kT)-1]^{-1} c\Delta\nu$ in a single longitudinal mode. By introducing aperture control on the angular extent of emission between succesive reduced gain stages, this contribution can be reduced but not eliminated entirely.

• ***Nonlinear Crystals for OPA Imaging***

Resolution and quality of image conversion in a parametric process is affected primarily by the angular aperture for phasematching and spatial uniformity of the gain distribution or space-bandwidth product as defined by the pump beam profile [19]. Amplifier operational characteristics should be optimized for both acceptance angle and overall gain efficiency. New materials with large nonlinear coefficients and less dispersion are needed to dramatically decrease angular selectivity and phasematching constraints, thereby increasing maximum image resolution (spatial frequency content) and dynamic range for detection. The optimization criteria for choice of nonlinear crystal should include a large nonlinear coefficient in the required phasematching configuration and a large tolerance to divergence of the pump beam to achieve a large acceptance angle. Nominal crystal interaction lengths in the amplifier should be designed to minimize spatial and temporal walk-off dispersion effects detrimental to gain conversion, and the input focussing geometry should use confocal parameters optimized for efficient spatial overlap, maximum interaction length, and angular acceptance bandwidth.

Double pass gate geometries or multiple walk-off compensated crystals oriented to reverse phase slippage between extraordinary and ordinary waves in the first crystal can be used to improve gain performance and simultaneously increase acceptance angle at the expense of alignment complexity. High gain and relaxed quasi-phasematched conditions over a wide field-of-view can be potentially accomplished in segmented or periodically poled waveguide structures in the near infrared. In some cases, spatial walk-off effects can be mitigated by operating in a non-critical phasematching geometry (input beam propagating at 90 degrees relative to the crystal optic axis) so that the angular acceptance of the crystal is higher which in turn allows tighter focusing to be used. Working near the degeneracy point in type I phasematching may be generally useful for polychromatic amplification applications such as time-resolved fluorescence spectroscopy where the phasematching conditions must be satisfied over a wide cone of spatial wavevectors centered on the pump direction [20]. The ability to scan crystal phasematching orientation over a broad range of wavelengths will facilitate gated imaging of a wide variety of spectroscopic signatures, including fluorescence, photoluminescence, and Raman scattering.

• ***Acceptance Angle***

Field-of-view of a nonlinear optical convertor such as an OPA is rigorously constrained by the phasematching requirements for gain. The acceptance angle $\Delta\theta$ associated with critically phasematched nonlinear mixing in a birefringent crystal is a measure of the tilt tolerance away from the perfect phasematching angle where $\Delta k=0$ and the angular dependence of the extraordinary refractive index in the critical plane which affects mixing efficiency. This angle varies inversely with crystal length and is derivable from the first null in the gain response function (Taylor series in Δk expanded about the phasematching angle) as:

$$\Delta\theta=(4\pi/L)(\partial\Delta k/\partial\theta)^{-1} \qquad (2)$$

Its magnitude will have important consequences for crystal walk-off effects, Fourier imaging, and performance of off-axis tangential and radial meridians of the incident light field in the optical tranfer function.

• ***Diffractive Imaging with Optical Parametric Amplification***

Imaging resolution characteristics of an optical parametric amplifier can be understood by considering the role of phasematching conditions in the spatial frequency domain [19,20]. Each spatial frequency in the amplified bi-dimensional image, represented as a set of signal fields with k-vectors at varying angles to the pump beam, can be associated with a plane wave that propagates in a particular direction in the nonlinear gating crystal. The distribution of spatial frequencies comprising the overall plane wave superposition is then mapped by coherent diffraction to an optical transfer function incorporating the phasematching bandwidth. Parametric amplification is restricted to a small range of k-vectors by phasematching which results in the formation of a passband in the transfer function. In this sense, an optical parametric amplifier acts as a "soft" confocal aperture for spatial amplification, with the gain passband rolling off with increasing Δk corresponding to higher-order diffraction orders of the signal relative to the pump direction. Plane waves corresponding to nonzero spatial frequency are not phasematched and experience less gain. By analogy to pinhole diffraction theory, the clear aperture (D) is defined by the focussing geometry optimized for crystal acceptance angle $\Delta\theta$, and the size of the gain region determines the spatial frequency cut-off $\nu_0 \sim D/f\lambda$ for image formation.

Transverse image resolution characteristics of an OPA are determined by the amplifier Fresnel number and the optical transfer function (OTF). The Fresnel number $N=(A/\lambda L)^2$ determines the number of resolution elements within the gain passband and since the gain of the gate is proportional to pump intensity (power over illumination area $A \sim D^2$), the number of resolution elements at fixed gain is ultimately determined by the pump power. The OTF describes the amplification and transfer of spatial frequencies in terms of phase mismatch, propagation vector, and crystal length [21]. Resolution and image conversion in a parametric process is affected primarily by the angular aperture for phasematching (acceptance angle) and the spatially-resolved gain distribution or space-bandwidth product. Therefore, one of the principle limitations of an OPA gate in imaging applications is the narrow angular acceptance imposed by the phasematching condition. This effect physically manifests itself when the OPA is located in an image plane by limiting resolution, and alternatively by limiting the useable FOV when it is placed in a pupil (transform) plane. Several solutions can improve on the angular selectivity of a phasematched interaction. One approach is to find new nonlinear materials with large nonlinear coefficients and less dispersion which are designed for noncritical phasematching (zero walk-off) or have a high Δk walk-off tolerance for gain, such as the case of quasi-phasematched materials (PPLN). Another approach is to walk-off compensate critically phasematched crystals with alternating birefringent axes so as to macroscopically approximate the noncritical phasematching condition; here the FOV increase is proportional to the number of crystal segments. A third approach which is not wavelength or material specific is to use discretized image synthesis with lenslet array structures.

• ***Optical Transfer Function***

Efficiency of amplification and transfer of spatial frequencies can be described by an optical transfer function (OTF) in terms of Δk mismatch, propagation vector, gain, and crystal length [21]. The optical transfer function formalism is a mechanism for image quality evaluation which provides a complete description of the object-image relation in terms of its effect on the Fourier decomposition of the object intensity pattern. In the context of optical systems theory, the OTF is the Fourier transform of the point spread representation of the energy distribution in the focal plane of an imaging system illuminated by a uniform plane wavefront.The gain passband in the transfer function of an OPA is defined by the convolution of the gain region, principally the pump spot size, and the phasematching acceptance bandwidth ~ $|\Delta k| < \pi/2L$. This passband acts as an apodizer in the full wavevector spectrum and establishes a direct linkage between angular phasematching condition and spatial resolution. As a result, when the OPA gate is placed in the Fourier transform plane of the image, the output field is limited in extent by the effective phasematching aperture and exhibits a resolution related to the lateral size of the pump beam; in a relay imaging configuration, the roles of the previous case are reversed and one can improve resolution at the expense field-of-view (FOV) by adjusting the overall magnification of the imaging system. Outside of this narrow region, transfer functions for both the signal and idler components are relatively constant over all spatial frequencies within the acceptance angle [22]. We directly measured the optical transfer function of spatial frequencies for the OPA by recording the Fourier plane image of a three-bar pattern with known periodicity through the imaging system. By moving the camera from the conjugate image plane to an image focal plane (FT plane), either an amplified image or its corresponding spatial frequency spectrum could be observed with suitable magnification. The spatial frequency response data can be normalized and compared to the theoretical idealized fitting function for the referenced distribution pattern. Slight astigmatism due to the orientation of the crystal walk-off plane will cause a difference in spatial resolution between vertical and horizontal directions in the viewing aspect.

• ***Coherent Image Processing***

Parametrically amplified ballistic imaging is capable of resolving a broad range of spatial frequencies and complex shapes with high fidelity and minimal phase distortion. In addition to performing direct image amplification, theoretical predictions made by several authors have shown that the optical parametric process can be used to selectively amplify the image spatial frequency distribution as a function of phase mismatch Δk. When the magnitude of Δk mismatch increases, maximum gain in the OTF will shift to higher spatial frequencies and the width of the passband narrows transitioning from a bandpass to an edge filter response characteristic. By manipulating the image-bearing field at the Fourier transform plane of the gate crystal relative to a nonuniform or prepatterned pump (gating) pulse, various plane wave components can be preferentially enhanced with respect to overall image intensity as a function of the gain coupling. In this mode of operation, the nonlinear gate can be configured as an active component for transmission and manipulation of optical information in coherent optical processing applications, including selective edge enhancement, character recognition, novelty filters, and correlation [21,22].

IV. PROOF-OF-CONCEPT DEMONSTRATIONS AND MODELING RESULTS

• ***Transillumination imaging of targets embedded in diffuse phantoms***

As a preliminary benchmark experiment, we have used time-gated femtosecond parametric amplification in a β-barium borate (BBO) type I ($e \rightarrow o+o$) crystal ($\theta=29^\circ$) to reconstruct and enhance infrared monochromatic transillumination test images with absolute feature sizes of 65 μm in background scattering attenuations exceeding 10^{12}. In our experimental system (described in detail elsewhere ref 23) , we cascaded two parametric amplifiers, one as a wavelength-tunable broadcast source, and the second as a ballistic gate after the test object. The interrogation wavelength could derived from either the signal or idler branches of the first OPA and both amplifier stages were pumped by second harmonic light derived from a regeneratively amplified titanium sapphire laser [24]. Two-dimensional amplified ballistic images of a standard Air Force resolution chart embedded between opal diffusers simulating random media were obtained for various attenuations and exposure times < 10s using a liquid nitrogen cooled 1024x1024 CCD detector array. These diffusers were basically nonabsorbing Lambertian scatterers which attenuate the useful component of the image-bearing light by randomizing the distribution of photon paths traversing the sample and by deflecting light (via multiple scattering) from the optic axis and field-of-view of the gate. Thus the effect of the diffuser is to both effectively attenuate the beam, and to completely obscure any underlying image information by producing a strong diffuse scattering afterglow. It should be emphasized that this process is an entirely different effect then simply attenuating the intact coherent beam; here the image is not recoverable with standard line-of-sight techniques (no pump). Images and corresponding lineouts produced with 10-100 nJ incident pulse energies at a 250 KHz repetition rate are displayed in the figures.The OPA transfer function was completely characterized and near-infrared transillumination images (λ~1.3 μm) were spectral upconverted with gain to visible wavelengths (~580 nm). Both Fourier and image plane geometries were explored.

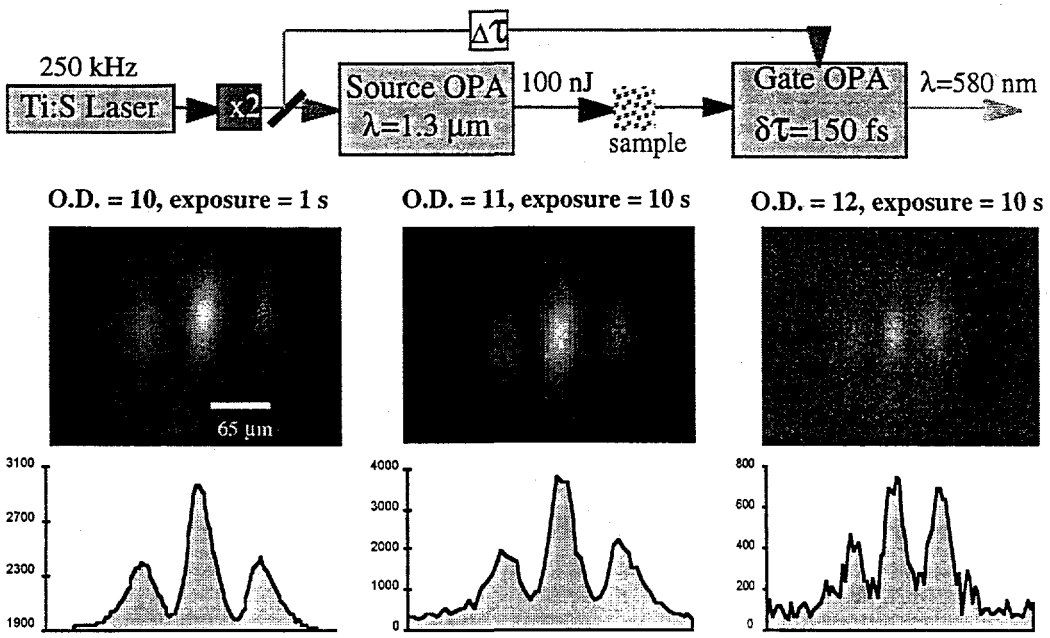

Figure 6: Laboratory demonstration of parametrically upconverted ballistic images using a wavelength-tunable cascaded OPA system shown above. The interrogated sample is a standard resolution chart embedded between Lambertian opal diffusers to create the stated optical density conditions. Scattering attenuation of 12 OD is representative of ~20 attenuation lengths (1/e) and a reflectivity of 10^{-4} which corresponds to a penetration depth ~ 1 km of cumulus cloud ($\kappa \sim 10^{-2}$ m^{-1}) or 10 m of Chesapeake Bay coastal sea water.

- ***Reflection Imaging of diffuse and specular targets through extended scattering media***

We examined the feasibility of using an OPA gate to detect and spatially resolve single-shot reflective images from specular, extended, and diffuse objects through coastal seawater and flame scattering environments emulating cloud cover or other obscurants. A test geometry was constructed in which a multipass cell was used to obtain long scattering pathlengths through turbid water. Two commercial Nd:YAG regenerative amplifiers, seeded by the same modelocked pulse train, were used to generate temporally synchronizable millijoule-energy gating (355 nm) and 50 μJ ranging (532 nm) pulses.

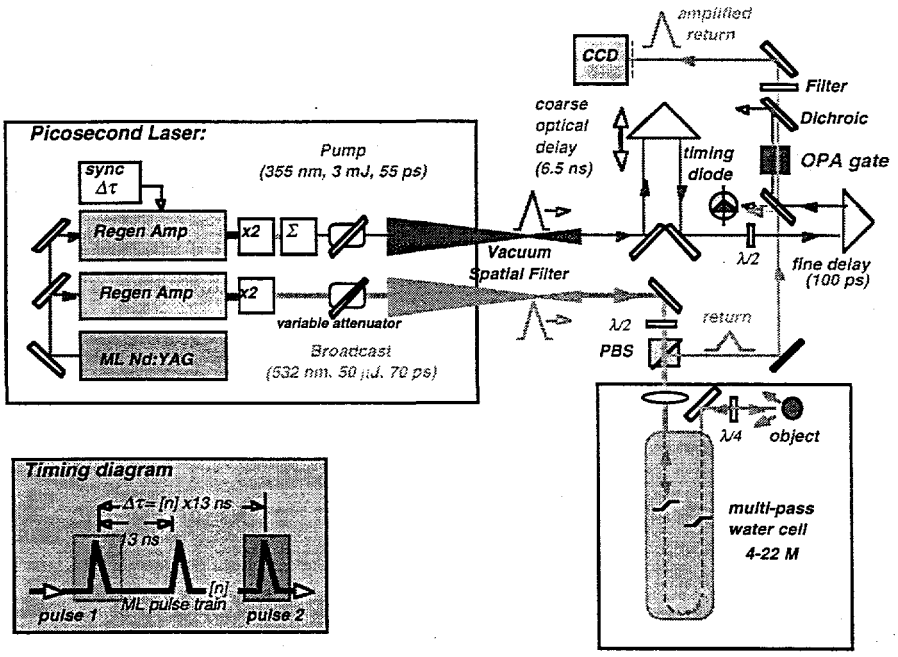

Figure 7: Proof-of-principle demonstration of range-gated reflection imaging through an extended scatterer using an OPA gate and electronically synchronizable regenerative amplifiers. The turbid media is a multipass water cell with Mylanta additive.

These pulses were subsequently overlapped spatially and temporally in the nonlinear optical gate to initiate ballistic image formation allowing for propagation delay and temporal dispersion in the broadcast arm. To accommodate extended range delays, alternate seed pulses (relative to probe) from the 76 MHz modelocked oscillator were switched into the pump amplifier in 13 ns increments and a short adjustable optical delay (6.5 ns max) was utilized to fine tune inter-pulse timing.

Specular and diffuse glints were detected single-shot (unaveraged) through a total pathlength of 8.8 m in water conditions emulating coastal seawater ($\kappa = .6\ m^{-1}$) with a dynamic range exceeding 10 OD. Note that in the diffuse reflectance case, the aperture of the final imaging/collection optic acts as a stop in the diverging return causing an effective attenuation of six orders of magnitude. True sub-millimeter range-gated 2-D imaging of standard resolution charts was performed through a scattering depth of $\gamma=\kappa L\sim 2$ corresponding to 1-2 km of cloud and the full OPA angular bandwidth (1 m EFL) was shown to support resolvable spatial frequencies > 10 cycles/mR without external angular magnification (eg, angle-angle imaging using the receiver aperture resolving capability). The required extent of frequencies matched to the OPA acceptance angle to visualize a target of minimum dimension *w* (meters) at range *R* (km) subject to line-pair rules (*N*) defining information content (detection, orientation, recognition, identification in ascending order) for a monochromatic display viewed by a human observer is given by *1.5 (N) x R/w*. One can decrease the number of line pairs for target identification with a priori knowledge of object characteristics from other supplemental sensors and by multispectral operation. Subpixel super-resolution methods can determine the angular location of a blur spot on the focal plane to an accuracy appoaching the optical resolution divided by the SNR using the method of centroids assuming active stabilization is operative.

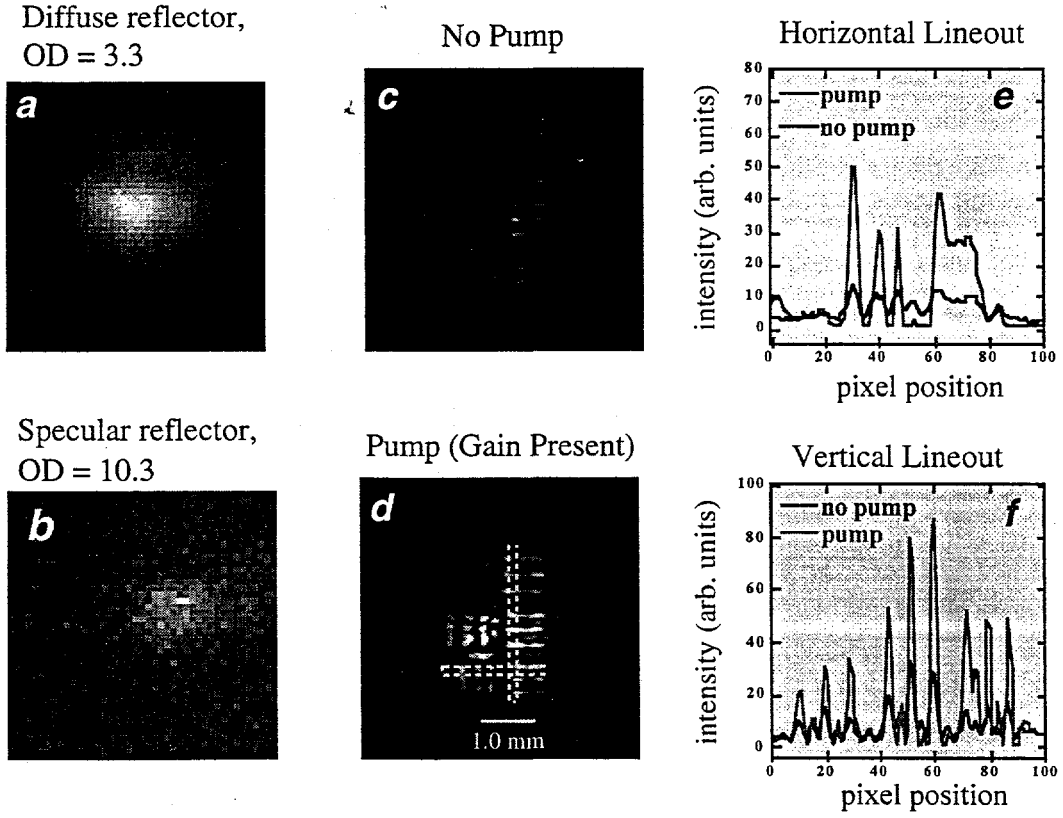

Figure 8: Amplified single-shot reflective glints in turbid water/Mylanta (8.8 meter pathlength): (a) return from diffuse Au reflector (38%) through scattering attenuation of 3.3 OD; (10^{-6} f-stop loss) (b) return from specular reflector (99%) through 10.3 OD. Range-gated OPA images and corresponding lineouts of Air Force resolution chart: (c) ungated image (no pump); (d) gated image; (e) horizontal line-out from dashed image region; (f) vertical line-out. No pump condition is superimposed for clarity. Note the presence of weak gain signatures from irregular glass substrate structure and multiple reflections.

The basic ability to segment an extended object in the range coordinate using a scanning delay in the OPA imaging process was verified using a distributed stack of partially reflecting mirrors at predetermined positions. Experiments are currently on-going to image true three-dimensional objects, rather than assemble two-dimensional projections, which is closely analogous to reflectance tomography. Shadowing and aspect geometry will be important variables in this case.

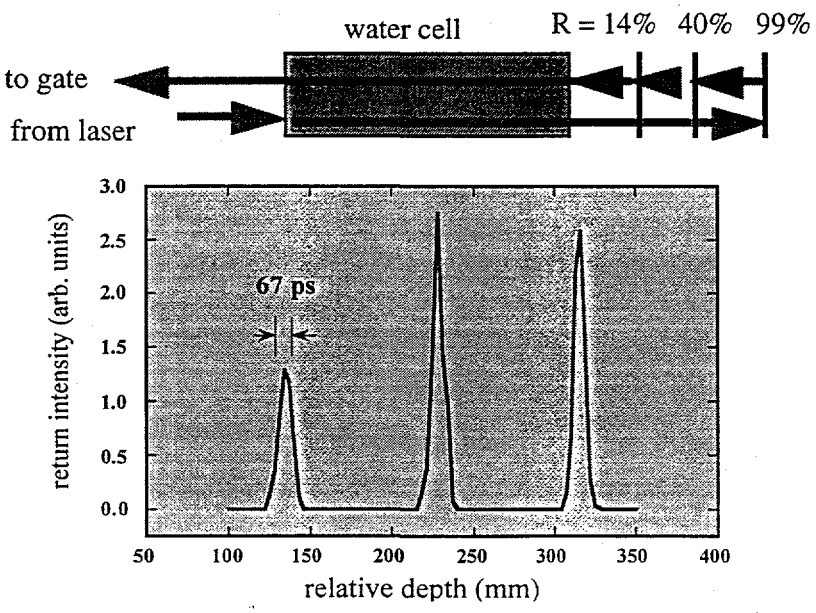

Figure 9: Range-gated glints from a series of obscured partial reflectors used to simulate an extended object.

A related experiment confirmed the applicability of this technique to the detection of objects obscured by turbulent flames and smoke. In these experiments, comparable spatial resolution was achieved in the presence of scattering attenuations of 10^8 and a 500C° flame, conditions for which standard thermal imaging and 3-5 μm infrared passive detection (PtSi FLIR) would fail. This demonstration shows that the gated optical imaging system is capable of nearly instantaneous battle damage assessment by virtue of high spatial resolution and relative immunity to thermal noise sources such as burning wreckage and optical turbidity in the visual field from collapsing dust debris. Since the measurement signal is optical, the theoretical response time is limited only by the light propagation delay back from the target.The unprecedented level of performance demonstrated by the OPA gate imaging approach in these instances exceeded any previous benchmarks published in the literature.

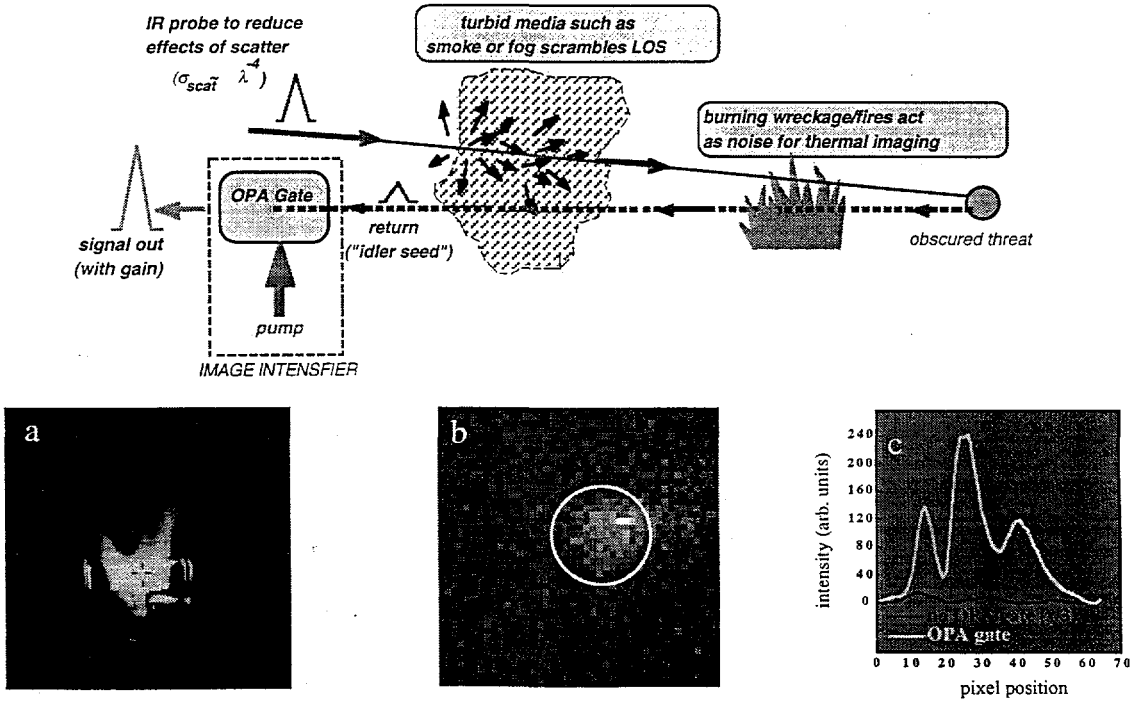

Figure 10: Basic OPA imaging configuration for penetrating smoke and flame. Experimental results: (a) 3-5 μm image with passive PtSi array; (b) amplified reflective glint obtained through OD=8 scattering attenuation; (c) line-out of imaged resolution chart (OD=2.3) exhibiting submillimeter (.7 mm) line separation contrasted with no gate.

- ***Detection of phase objects in turbidity***

Hartmann sensing offers a simple method for measuring the optical phase and intensity of laser light that has been transmitted through an aberrating medium without recourse to interferometry [25,26]. In general, a Hartmann sensor consists of lenslet array with focal length (f), a pixelated camera, and a centroid algorithm that can accurately locate the positions of focal spot intensity patterns recorded by the camera. The impinging wavefront field is dissected by an array of transmissive lenslets $\{i\}$ which focus the incoming light within each subaperture onto the image plane. The sensor works on the principle that focused spots x_{ij} in the back focal plane of the microlens array will be deflected a distance $\delta=x_{ij}-x_{i0}$ away from their respective optical axes due to aberrations in the optical beam. For a given incoming spherical wave the measured tilt is approximately a linear function of position along the sensor array for small-angle sampling. Because light propagates in a direction normal to the wavefront, the deflection distance is proportional to the local derivative or slope $\theta\sim\delta/f$ of the optical wave front impinging on the lenslet array. Detecting the centroid position measures the gradient of optical phase along the detector axis which can subsequently be integrated to yield the optical phase distortion experienced by the beam relative to a calibration file. A digital phase reconstruction algorithm can be utilized to construct a map of complex field phasors defining the full phase front $\phi(j)$ across the measurement aperture and associated moments can be projected on a Zernike polynomial basis set. Sensitivity of the Hartmann sensor is determined by the smallest tilt differential $\Delta\theta$ that the sensor can measure between successive lenslets. Knowing the complete scalar field of the beam will facilitate detailed predictions of actual beam characteristics along its propagation path through the intervening medium.

Low-contrast phase objects masked by turbid backgrounds were ballistically detected with a maximum OPD sensitivity approaching $\lambda/100$ using a binary-optics based Shack-Hartmann wavefront sensor in combination with the parametric amplification time-gate process.Standard interferometric methods for detection of phase are seriously degraded in the presence of diffuse scattering and would not be able to distinguish such objects normally. Image reconstruction (phase and amplitude) of the obscured object were accomplished by performing precise wavefront sensing on the ballistically gated coherent field to determine the local gradient of phase, i.e., by monitoring the centroid location of lenslet image spots in the back focal plane. This phase measurement capability is a useful complement to ballistic imaging when refractive index variation $\Delta n/n$ dominates the optical response- translucent objects, wake field, thermoclines, shear boundaries. It is also the basis for combining adaptive optics with the OPA imaging approach to simultaneously compensate for the effects of atmospheric turbulence and turbidity on image resolution. Previous attempts to do turbulence compensation in strong scattering situations have produced anomalous results because of poor wavefront estimators in the reconstructor.

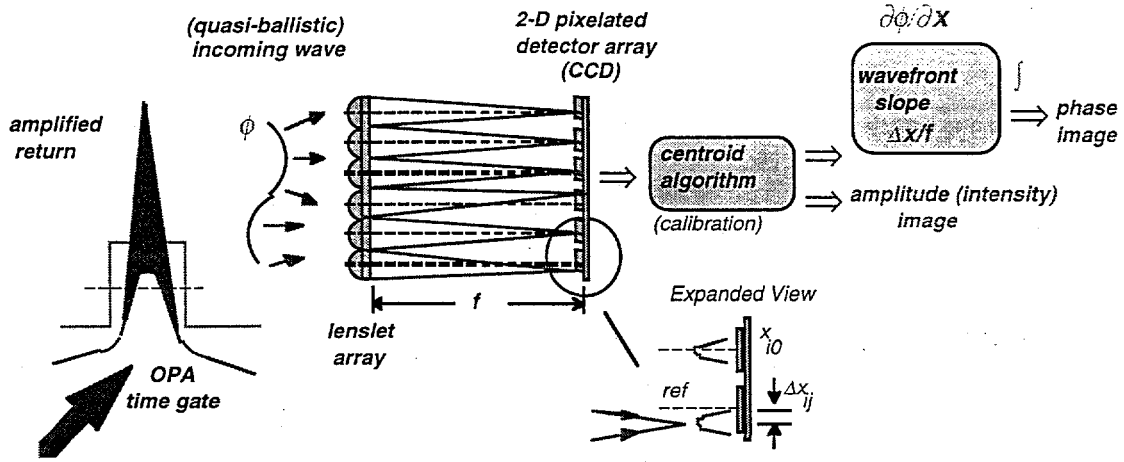

Figure 11: Simultaneous intensity and phase imaging of obscured or weak emission signatures can be achieved by integrating time-gating with an optical parametric amplifier and Shack-Hartmann wavefront sensing based on a binary-optics lenslet array.

As an experimental test, we reconstructed transillumination phase front and intensity contour plots of a weak 2 meter radius of curvature negative field lens placed in front of a diffuser with overall optical density OD=4 using a 40x32 lenslet array (250 μm pixel diameter). The path delay in the time-gate was adjusted for the average thickness of the test lens and the overall magnification of the composite optical system allowing for field lens defocussing did not significantly perturb the crystal gain conditions. By incorporating this capability to measure the wavefront slope (phase gradient) and amplitude of range-gated OPA output, it is possible to simultaneously acquire phase and intensity maps of the dielectric function of an obscured object.

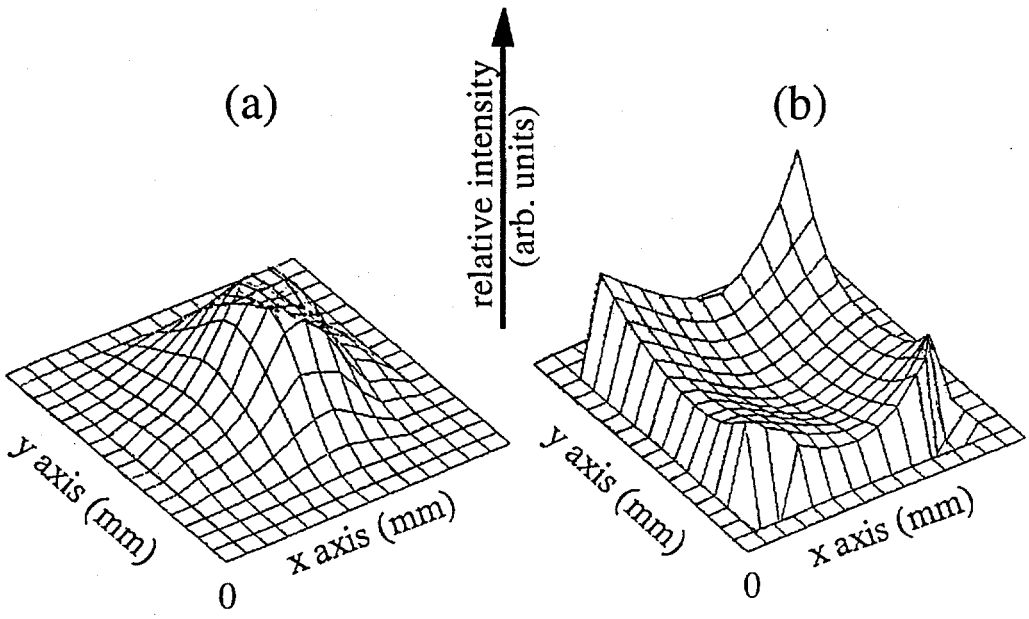

Figure 12: Detection of a weak negative lens obscured by scattering; (a) intensity distribution; (b) phase variation due to lens curvature across wavefront.

• ***Modeling results for penetrability of cloud cover and obscurants***

Comprehensive analysis of imaging radar performance will require detailed statistical analysis of correlated effects of atmospheric attenuation (Huygens-Fresnel) and tubulence strength (Kolmogorov) along the propagation path combined with specific electromagnetic scattering models for target reflection. A complete evaluation of look-down simulated imagery would include the effects of scintillation, speckle, background clutter, and additive noise effects on each pixel using a realistic weather model. As a preliminary estimate of capabilities for a monostatic OPA system in various scattering environments, we used first-principles laser radar equations in conjunction with our measured experimental data and reasonable extrapolating assumptions for radiometric margin and target type. In these calculations, a standard mid-latitute daytime atmospheric model was assumed and the diffusely reflective target was considered as fully intercepted with diffraction loss governed by an inverse range dependent power law $1/R^2$. The hypothetical diffuse target, as distinguished from a probabilistic distribution of specular facets, is presumed to be imaged against a background of nonzero spatially uniform average reflectance within the range resolution cell where the primary fluctuations are due to turbulence scintillation and speckle. Spatial, spectral, morphological, and temporal bandpass filtering in the OPA can all be used to reduce the effects of unwanted background noise and stationary clutter artifacts in the viewing scene. Speckle reduction is assumed to be acomplished with advanced post-processing algorithms for bispectral-based reconstruction and time-averaged frame-differencing techniques.

The basic operative lidar equation used to calculate various properties of the OPA imaging system was

$$I = I_o A \rho / 4\pi L^2 \ exp\ (-2\kappa L) \qquad (3)$$

where I_O is the laser energy, A is the collector area, ρ is the target reflectivity, $\mathcal{L}$ is the range and κ is the extinction coefficient due to scatter and absorption. This equation assumes that the intensity of the ballistic component obeys an exponential attenuation law and is purely monopath. All the light received by the collector is assumed optimally relayed with angular magnification to within the acceptance angle of the OPA crystal and the pump spot diameter; size of the broadcast laser spot on target matches the collector/crystal field of view. When the energy of the broadcast laser is margined for offsetting scattering and range losses, the gain, which is determined to first order by the pump intensity, remains fixed just below the optical parametric noise limit corresponding to the minimum useable detectable signal measured in the laboratory ~10^{-15} J subject to a SNR=6 baseline. In the range contour plot, the system size defined as the product of broadcast energy times collection aperture is held constant as a function of scattering extinction and target reflectivity, and the turbidity is conservatively assumed to exist along the entire scattering path (i.e., range and pathlength are the same). Representative oceanographic and atmospheric scattering properties are included for reference. Note that in most realistic remote sensing scenarios, the optical depth

of the scattering layer is significantly less than the range or porosity may exist (cloud cover). Margin calculations relating system size to optical depth and detectable range for fixed SNR threshold and target reflectivity have also been developed for engineering considerations.

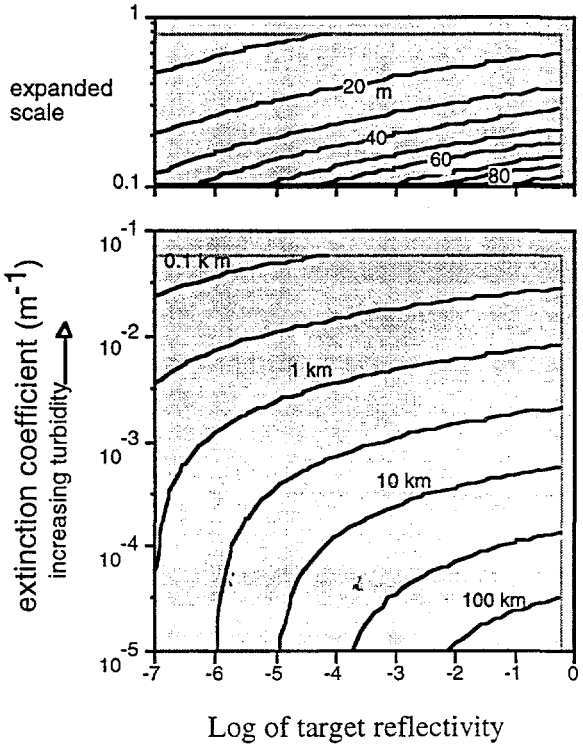

Figure 13: Maximum range contours as a function of target reflectivity and scattering loss for the minimum single-shot detectable signal as scaled to the laboratory system. Scattering is assumed continuous between source and target; system size 100 mJ*m^2.

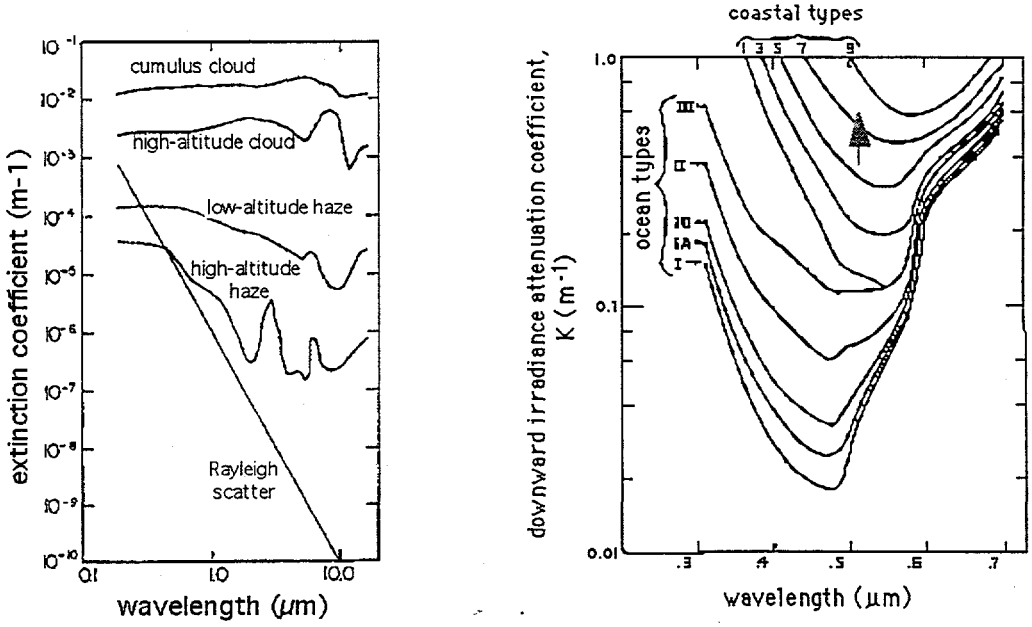

Figure 14: Scattering coefficients for various atmospheric phenomena and water types [27].

V. CONCLUSIONS

Optical parametric gating represents an important application of nonlinear optics to the ranging and visualization of objects obscured by scattering which are not observable using conventional line-of-sight optical remote sensing techniques. Summarizing the salient operational advantages of a time-gated OPA image intensifier for laser radar applications:

- versatile all-optical component integrating gain, wavelength, and gating functions
- short variable gate duration for maximum range resolution, image contrast, and diffuse light rejection
- high transmission efficiency with unsaturated amplification (gain) $>10^5$
- demonstrated dynamic range ($>10^{10}$) for image capture in low-visibility scattering environments
- phasematched nonlinear process offers simultaneous spatial, temporal, spectral, and polarization discrimination
- broad wavelength tunability from near ultraviolet to mid-infrared with existing laser sources and crystals
- image amplification and frequency conversion to separately optimize detector and propagation properties
- compatible with wavefront sensors and coherent optical processing operations in the transform plane

VI. ACKNOWLEDGEMENTS

Support for this research was provided under a contract with the Department of Energy at Sandia National Laboratories DE-AC04-94AL85000. The authors wish to acknowledge invaluable scientific discussions with Dr. Steven Wilkinson, Dr. Maurice Halmos, and Dr. David Fink at Raytheon Systems Corporation (El Segundo, CA) regarding the operation of contemporary laser radar systems.

VII. REFERENCES

1. K.M. Yoo and R.R. Alfano, "Time-resolved coherent and incoherent components of the forward light scattering in random media," Optics Letters, vol. 15, p. 320, 1990.

2. L. Wang, P.P. Ho, C. Liu, G. Zhang, and R.R. Alfano, "Ballistic 2-D imaging through scattering walls using an ultrafast optical Kerr gate," Science, vol. 253, p. 769, 1991.

3. S.C.W. Hyde, N.P. Barry, R. Jones, J.C. Dainty, P.M.W. French, M.B. Klein, and B.A. Wechsler, "Depth-resolved holographic imaging through scattering media by photorefraction," Optics Letters, vol. 20, p. 1331, 1995.

4. J.A. Moon, R. Mahon, M.D. Duncan, and J. Reintjes, "Three-dimensional reflective image reconstruction through a scattering medium based on time-gated Raman amplification," Optics Letters, vol. 19, p. 1234, 1994.

5. N.H. Abramson and K.K. Spears, "Single pulse light-in-flight recording by holography," Applied Optics, vol. 28, p. 1834, 1989.

6. M. Toida, M. Kondo, T. Ichimura, and H. Inaba, "Two-dimensional coherent detection imaging in multiple scattering media based on directional resolution capabilities of the optical heterodyne method," Applied Physics, vol. B, 1991. Also: M.R. Hee, J.A. Izatt, J.M. Jacobson, and J.G. Fujimoto, "Femtosecond transillumination optical coherence tomography," Optics Letters, vol. 18, p. 950 (1993).

7. J.C. Hebden and K.S. Wong, "Time-resolved optical tomography," Applied Optics, vol. 32, p. 372 (1993).

8. S. Andersson-Engels, R. Berg, S. Svanberg, and O. Jarlman, "Time-resolved transillumination for medical diagnostics," Optics Letters, vol. 15, p. 1179, 1990.

9. G.W. Faris and M. Banks, "Upconverting time gate for imaging through highly scattering media," Optics Letters, vol. 19, p. 1813, 1994.

10. J. Watson, P. Georges, T. Lepine, B. Alonzi, and A. Brun, "Imaging in diffuse media with ultrafast degenerate optical parametric amplifier," Optics Letters, vol. 20, p. 231, 1995.

11. S.M. Cameron, D.E. Bliss, and M.W. Kimmel, "Gated frequency-resolved optical imaging with an optical parametric amplifier for medical applications,"SPIE, vol. 2679, p. 195, 1996.

12. J.J. Zayhowski and C.Dill III, Optics Letters, vol. 20, p. 716, 1995.

13. G.M. Loubriel, F.J. Zutavern, A.G. Baca, H.P. Hjalmarson, T.A. Plut, W.D. Helgeson, M.W. O'Malley, M.H. Ruebush, and D.J. Brown, "Photoconductive semiconductor switches," IEEE Transactions on Plasma Science, vol. 25, p. 124, 1997.

14. U.J. Greiner and H.H. Klingenberg, "Picosecond intracavity optical parametric oscillator," Optics Letters, vol. 22, p. 43, 1997.

15. M.J. Halmos and J.H.S. Wang, "Laser radar systems and applications," Optical Technologies for Aerospace Sensing, Critical Reviews of Optical Science and Technology, vol. CR47, p. 308, 1992. Also: J.A. Overbeck, M.S. Salisbury, M.B. Mark, and E.A. Watson, "Required energy for a laser radar system incorporating a fiber amplifier or an avalanche photodiode," Applied Optics, vol. 34, p. 7724, 1995.

16. J.C. Hebden, "Evaluating the spatial resolution performance of a time-resolved imaging system," Medical Physics, vol. 19, p. 1081, 1992.

17. E.B. de Haller, C. Depeursinge, and C.Y. Genton, "Resolution of time-resolved breast transillumination in vitro measurement compared with theoretical predictions," Optical Engineering, vol. 34, p. 2084, 1995.

18. F. Zernike and J. E. Midwinter, Applied Nonlinear Optics, John Wiley and Sons, New York, 1973.

19. A. Gavrielides, P. Peterson, and D. Cardimona, "Diffractive imaging in three-wave interactions," J. Applied Physics, vol. 62, p. 2640, 1987.

20. F. Deraux and E. Lantz, "Parametric amplification of a polychromatic image," JOSA, vol. B12, p. 2245, 1995.

21. F. Deraux ans E. Lantz, "Transfer function of spatial frequencies in parametric image amplification: experimental analysis and application to picosecond spatial filtering," Optics Communications, vol. 114, p. 225, 1995.

22. P.A. Laferriere, C.J. Wetlerer, L.P. Schelonka, and M.A. Kramer, "Spatial frequency selection using down-conversion optical parametric amplification," Applied Physics, vol. 65, p. 3347, 1989.

23. S.M. Cameron and D.E. Bliss, "Gated frequency-resolved optical imaging with an optical parametric amplifier for medical applications," Sandia Report, SAND97-0234, UC-906, 1997.

24. M.K. Reed, M.K. Steiner-Shepard, M.S. Armas, and D.K. Negus, "Micro-joule ultrafast optical parametric amplifier," JOSA, vol. B12, p. 2229, 1995.

25. L. McMackin, B. Masson, N. Clark, K. Bishop, R. Pierson, and E. Chen, "Hartmann wavefront sensor studies of dynamic organized structures in flow fields," AIAA Journal, vol. 33, p. 2158, 1995.

26. D.R. Neal, J.D. Mansell, J.K. Gruetzner, R. Morgan, and M.E. Warren, "Specialized wavefront sensor for adaptive optics," SPIE Proceedings Adaptive Optical Systems and Applications, vol. 2534, p. 338, 1995.

27. Measures, Remote Sensing, John Wiley and Sons.